COMPOSITION AND MICROFACIES OF ARCHEAN MICROBIAL MATS (MOODIES GROUP, CA. 3.22 GA, SOUTH AFRICA)

ANTONIA GAMPER, CHRISTOPH HEUBECK, AND DIETER DEMSKE

Freie Universität Berlin, Institute of Geological Sciences, Malteserstraße 74-100, 12249 Berlin, Germany
e-mail: antonia.gamper@fu-berlin.de

AND

MAREK HOEHSE

Bundesanstalt für Materialforschung und-prüfung (BAM), Richard-Willstätter-Straße 11, 12489 Berlin, Germany

ABSTRACT: The Middle Archean Moodies Group (ca. 3.22 Ga), Barberton Greenstone Belt, South Africa, exposes one of the world's oldest ecosystems. It includes kerogen-rich laminae and thin chert bands interbedded with coarse-grained and gravelly sandstones. The strata record a medium-energy, tidal coastal environment. Analyses of the microscopic structure and chemical composition of the chert bands through petrographic microscopy, Raman microspectroscopy, laser-induced breakdown spectroscopy (LIBS) analyses, C isotopes, and scanning electron microscope (SEM) photography of macerated material, supported by textural observations of hand samples, suggest that these laminae represent variably compressed and early-silicified microbial mats.

Internal wavy laminations, amorphous carbon composition, and negative δ^{13}C values strongly imply a biogenic origin. Complete HF maceration of chert bands revealed polygonal cell structures in a formerly extracellular polymeric substance matrix. The tuft- and dome-micromorphology of the laminations resembles that of recent photosynthetic filament-dominated microbial mats. Facies interpretations indicate that microbial mats extensively colonized subtidal to intertidal Archean siliciclastic coastlines.

KEY WORDS: Archean, Barberton Greenstone Belt, Moodies Group, microbial mats, tidal, MISS

INTRODUCTION

One of the most controversial issues in geobiology is the distinction between sedimentary structures of biogenic and abiogenic origin in Archean rocks (Altermann 2001, Altermann and Kazmierczak 2003, Brasier et al. 2006). Because pervasive physical and chemical alteration has widely affected the Archean sedimentary record, care must be taken to document the evidence for biogenicity of the oldest microorganisms, their metabolisms, and their interaction with the geo-, hydro-, and atmosphere. Whereas shallow-water microbial communities have been described from cherts, carbonates, and silicified evaporites of the ca. 3.4 Ga Strelley Pool Formation of Australia's Pilbara Craton (Ueno et al. 2001, Allwood et al. 2007, Marshall et al. 2007, Sugitani et al. 2010), the occurrences described here from the 3.22 Ga Moodies Group of the Barberton Greenstone Belt, South Africa, constitute the world's oldest known mappable biofacies in a shallow-water siliciclastic environment (Noffke et al. 2006, Heubeck 2009, Javaux et al. 2010). We here present field, microscopic, spectroscopic, and geochemical observations from the Moodies Group sandstones. Our results suggest that thick and resilient microbial mats may have been widespread in siliciclastic sub- to intertidal settings along flat Archean coasts.

REGIONAL GEOLOGY AND DEPOSITIONAL SETTING OF THE MOODIES GROUP

The ca. 3.5 to ca. 3.1 Ga Barberton Greenstone Belt (BGB; Fig. 1) of South Africa and Swaziland is one of the world's oldest well-preserved Archean greenstone belts. The BGB fill comprises the NE-SW–striking Barberton Supergroup (Brandl et al. 2006), which consists of, from base to top, the Onverwacht, Fig Tree, and Moodies Group (Anhaeusser 1976).

The Onverwacht Group is composed of predominantly ultramafic and mafic volcanic rocks, including felsic pyroclastic and volcaniclastic rocks and chert, while the Fig Tree Group mostly represents a deep- to shallow-marine environment and consists of graywacke, shale,
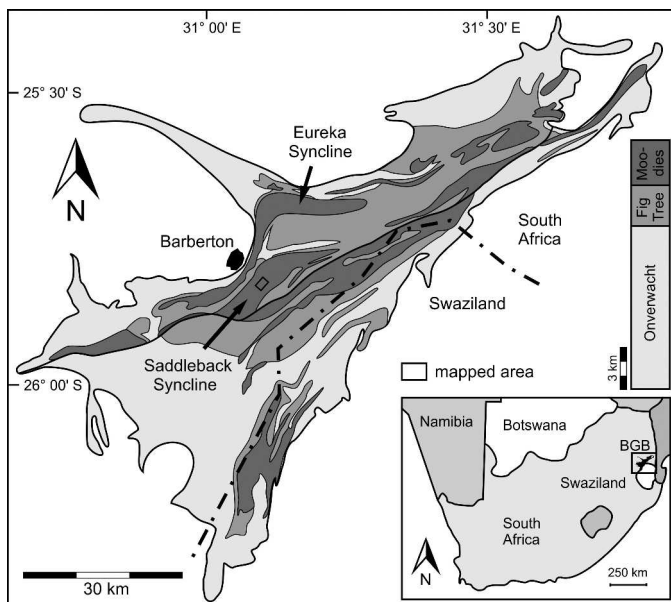

FIG. 1.—Geological sketch map of the Barberton Greenstone Belt (modified after de Ronde and de Wit 1994). Moodies Group strata occur in large synclines. The study area is located on the overturned southeastern limb of the Saddleback Syncline, marked by a black rectangle.
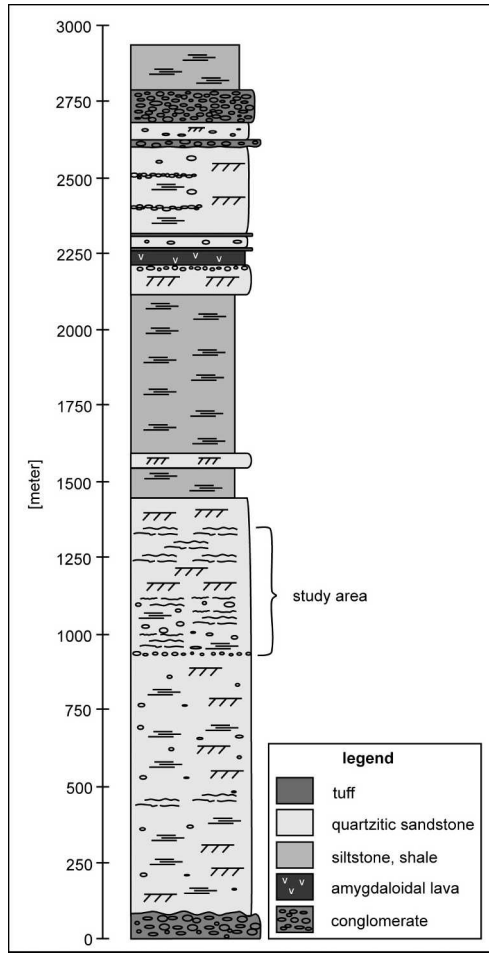
Fig. 2.—Standard stratigraphic column of the ~3200-m-thick Moodies Group of the Saddleback Syncline (Ohnemueller et al. 2010), including the sampled unit MdQ1 near its base. Anhaeusser (1976) defined the MdQ1 unit lithologically as coarse- and medium-grained, shallow-water, immature, quartzose sandstones.

banded iron formation, chert, basaltic lava, and ash-fall tuffs. The overlying Moodies Group mainly consists of lithic, feldspathic, and quartz-rich sandstones, which are locally interbedded with conglomerates, and reaches ~3200 m thickness in the Eureka Syncline. Shale, siltstone, volcanic units, and jasper are rare (Hall 1918; Visser et al. 1956; Anhaeusser 1975; Eriksson 1977, 1978, 1979, 1980; Heubeck and Lowe 1994a, 1994b; Heubeck and Lowe 1999; Lowe and Byerly 2007). Moodies strata (Fig. 2) were deposited in alluvial, fluvial, deltaic, tidal, and shallow-marine environments. They record the erosion of quartz-rich plutonic source rocks for the first time in Earth's history.

At several Moodies outcrop localities, well-preserved tidal bundles attest to an excellent degree of temporal resolution of the rock record at outcrop scale (Eriksson and Simpson 2002, Eriksson et al. 2006). Heubeck and Lowe (1994a) interpreted petrographic and textural trends in the lower Moodies Group as passive-margin– or rift-related environments, while the composition and architecture of the upper Moodies Group were interpreted as a response to syndepositional up-to-the-north faulting along the northern margin of the BGB, incipient basin uplift, and inversion in the context of overall greenstone belt

shortening. Moodies sedimentation began between 3.225 and 3.222 Ga and may have been only a few million years in duration (Heubeck and Lowe 1994a, Heubeck et al. 2010).

SETTING AND MACROSCOPIC STRUCTURES OF MICROBIAL MATS

Moodies Group strata dip steeply to subvertically on the overturned limb of the Saddleback Syncline in the central BGB (Fig. 1). There,
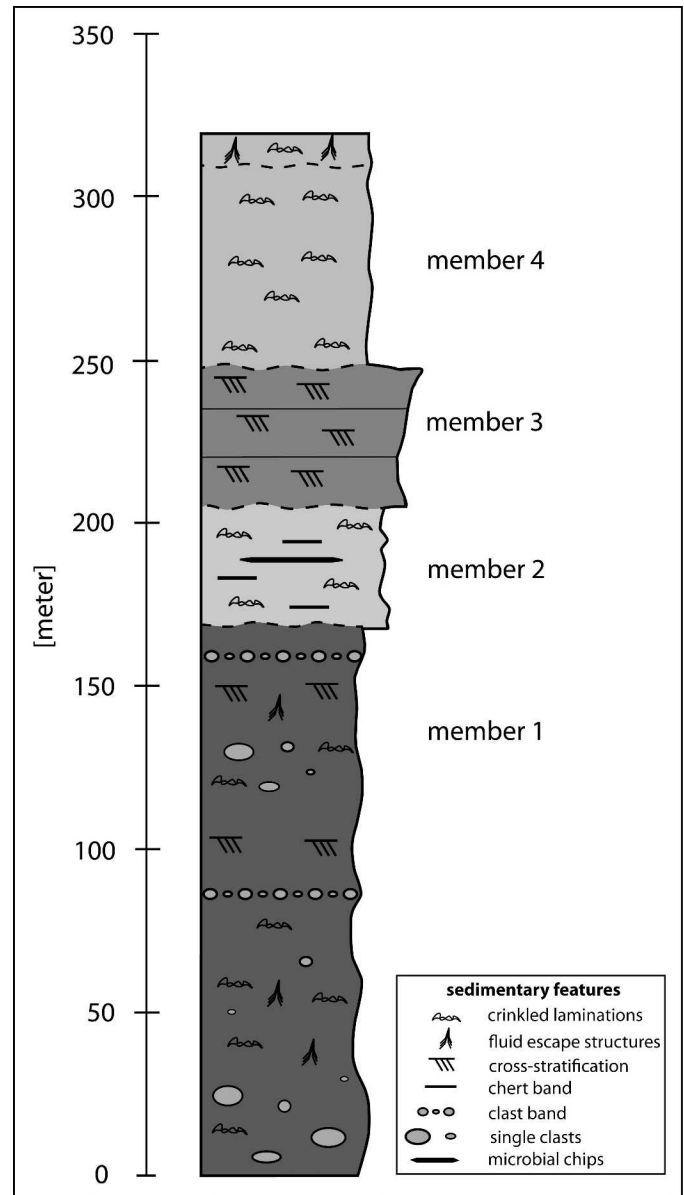

Fig. 3.—Detailed stratigraphic column of the studied area. Unit MdQ1 can be subdivided into at least four members (cf. Table 1). Facies are deepening-upward and represent a transition from terrestrial coastal environment (member 1) to a nearshore facies (member 4). Microbial mats are present in members 1, 2, and 4 and are absent in member 3. All strata show a NW-SE trend and dip subvertically at approximately 70°.

TABLE 1.—Sedimentary characteristics of the principal mapped units at the top of unit MdQ1.

Member	Lithology	Sedimentary structures	Facies interpretation
4 (top)	medium- to coarse-grained sandstone	- thin (1–3 mm), wavy, dark-green laminations with tuft and dome morphology - fluid escape structures - parallel stratification	nearshore (5–15-m water depth)
3	medium-grained sandstone	- large-scale cross-bedding (height ~2 m) - rare small-scale low-angle cross-bedding (height ~20 cm)	nearshore (5–10-m water depth)
2	medium- to coarse-grained sandstone, microbial-chip–clast conglomerate	- thin chert bands - parallel stratification - shallow but wide erosional scours	subtidal to intertidal
1 (base)	medium- to coarse-grained sandstone with single-clast gravel bands and single clasts	- small-scale low-angle cross-bedding - wavy, dark-green laminations, chert bands - single-clast bands (diameter 2–4 cm) - gravelly to pebbly conglomerate stringers - fluid escape structures - ripples and cross-beds - parallel stratification	terrestrial coastal

feldspathic and quartzose sandstones (unit MdQ1 of Anhaeusser 1976), with subordinate conglomerates, reach several hundred meters in thickness (Fig. 2) and include the microbial mat features described herein.

Unit MdQ1 (Fig. 2, bracket), ~300 m thick, is largely silica cemented, crops out resistantly, and can be followed over 11 km along strike. It marks a fluvial–marine transition (Eriksson et al. 2006). Siltstone, shale, or sedimentary structures related to suspension settling or desiccation and indicative of a low-energy environment (Eriksson 1978, 1979; Eriksson et al. 2006; Noffke et al. 2006) are absent. Noffke et al. (2006) described wrinkle structures and a single roll-up structure interpreted as a microbial mat from a stratigraphically equivalent section in the adjacent Dycedale Syncline. Javaux et al. (2010) documented large (~31–300 μm) organic-walled spheroidal micro-fossils in gray shales and siltstones from subsurface samples of the lower Moodies Group.

Detailed mapping (1:2500 scale) of a well-exposed part of unit MdQ1 in the Saddleback Syncline, extending approximately 2 km along strike, demonstrates that the mapped area includes four members, likely representing terrestrial coastal, low-angle shoreline, intertidal to subtidal, and nearshore facies (Fig. 3; Table 1). This study
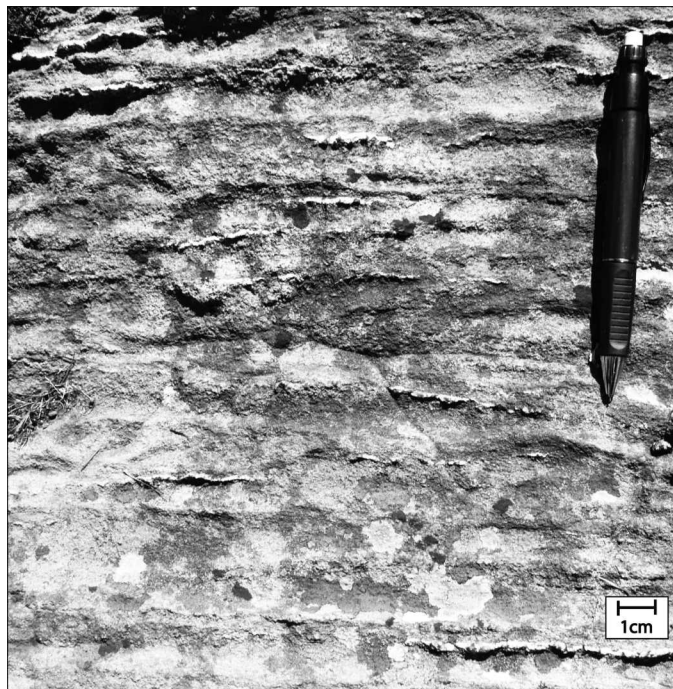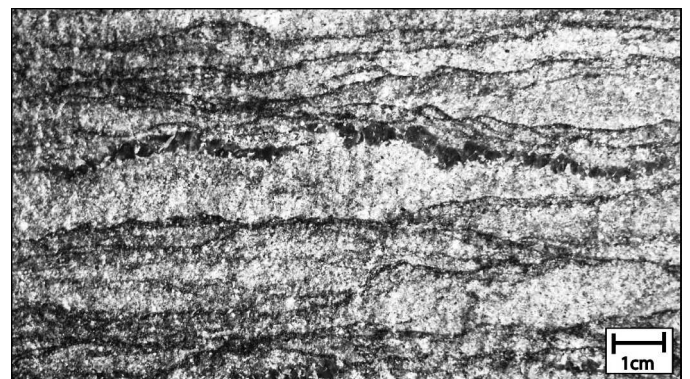

FIG. 4.—Outcrop photograph of Moodies medium-grained sandstone with indistinct, closely spaced crinkly laminations separating thin sand beds of varying grain size. Chert bands weather white and resistantly; they grade into the crinkly laminations and are parallel to bedding surfaces.

FIG. 5.—Black chert band, ~4 mm thick, associated with abundant thin wavy ("crinkled") laminations in a medium-grained sandstone of likely tidal to subtidal facies. Chert bands commonly (but not exclusively) occur on top of coarse-grained sand lenses. On a microscale, they show a convolute contact to the sand lens below but a smoother contact to overlying fine- to medium-grained sandstone (see also Fig. 6).
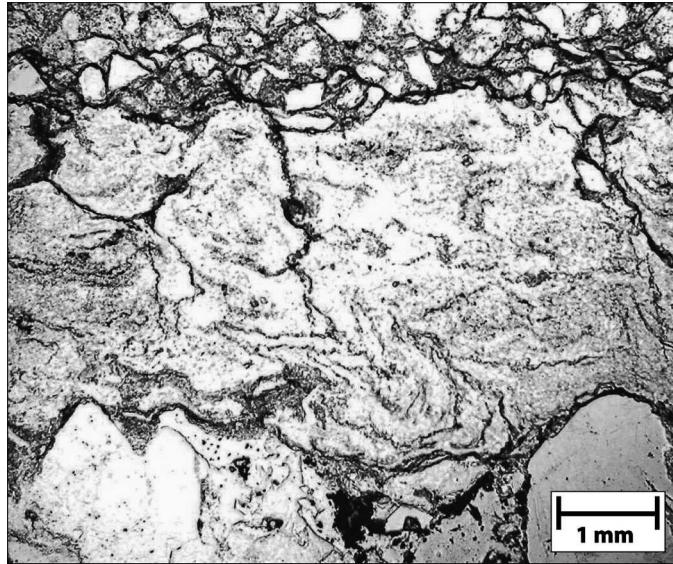
FIG. 6.—Photomicrograph of black chert band, 4 to 7 mm thick (center), perpendicular to bedding between medium- and coarse-grained sandstone at the top and bottom, respectively. Note multiple and parallel crinkled laminations defined by opaque matter.

METHODS

For assessing textural relations, slabs of fresh biolaminated sandstone samples with chert bands were cut perpendicular to the bedding and polished. Thin sections were prepared to identify petrographic composition and to study the internal morphology of the chert bands.

Carbonaceous material was identified using a scanning electron microscope (Zeiss Supra 40VP). One thin section and several small (size ~2 by 2 by 1 cm) chips were polished with silicon carbide and cleaned in distilled water using an ultrasonic bath. After flaming with alcohol in order to remove organic contaminants, sample chips were bathed in HCl to remove carbonates and then etched for 6, 10, 15, 20, or 30 minutes in 5% HF. Additional samples were partly (28 days) or completely (48 days) macerated in 50% HF, including two hot applications. HCl-washed residual material was heavy-liquid separated using $ZnCl_2$ (1.88 g/cm^3) to remove all nondissolved heavy minerals. This step was preceded and followed by fine sieving through 7-μm-mesh tissue. All samples were coated with gold prior to scanning electron microscope (SEM) analyses.

Molecular mapping experiments were conducted directly on the polished surface of the thin sections with a Raman microscope (LabRAM HR800, Jobin Yvon, Bensheim, Germany; Olympus BX41 microscope) equipped with an argon ion laser at an excitation wavelength of 488 nm (Melles Griot, Aalsbergen, Netherlands).

The elemental mapping on surface-polished chips was performed by laser-induced breakdown spectroscopy (LIBS). The experimental design has been described by Hoehse et al. (2009). In brief, a frequency-doubled pulsed Nd:YAG laser (Surelite II, Continuum, Germany) is focused on the sample. Some hundred nanograms of matter are evaporated and heated, followed by plasma generation. Plasma emission is collected with an Echelle spectrometer (Aryelle Butterfly, LTB Lasertechnik Berlin GmbH, Germany) in the range of 290 to 930 nm.

focuses on abundant, closely spaced, dark-green-weathering, crinkly and anastomosing laminations in the inter- to subtidal facies (member 2) and to a lesser degree in members 1 and 4 (Heubeck 2009) of the mapped area. Many crinkly laminations pass laterally into thin, black chert bands. The occurrence of these chert bands is mostly restricted to the shoreline facies (Table 1).
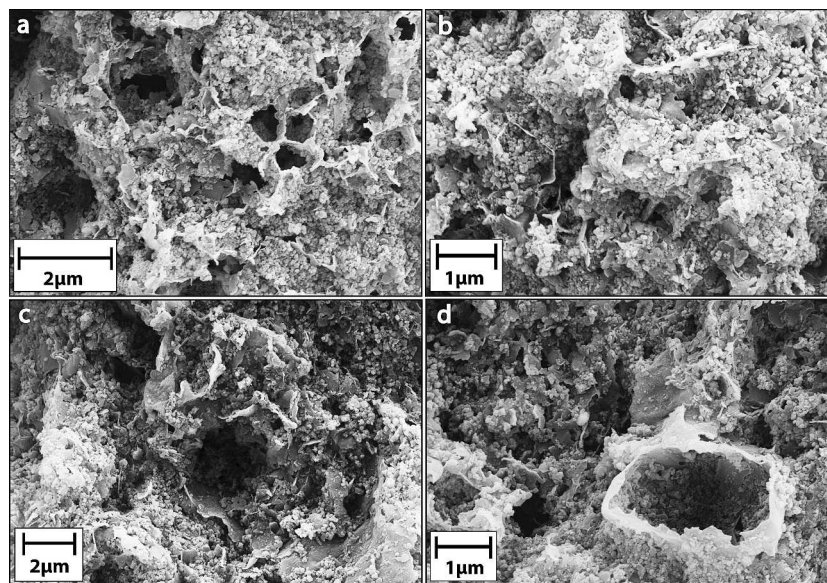

FIG. 7.—SEM photographs of partially macerated chert bands, exposed to 40% and 50% HF for 28 days. Observed structures are still partly embedded in silica matrix. The photographs show three-dimensional networks of likely microbial-mat origin, largely composed of polygonal cells with a diameter of ~1 to 2 μm. Some cavities are in part rounded, suggesting a biological origin; others are in part angular and may represent originally "floating" and now dissolved siliciclastic grains.
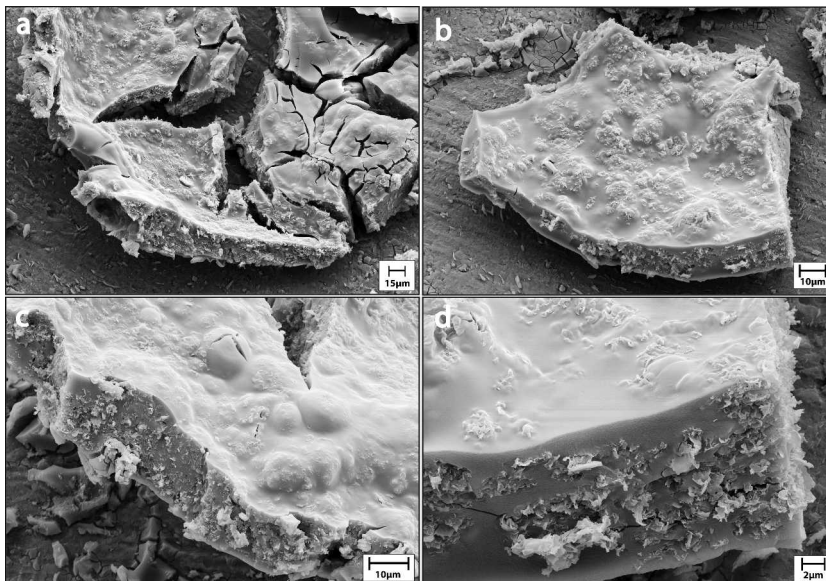
FIG. 8.—SEM images of carbonaceous fragments remaining after chips of dark chert were completely macerated using 50% HF for 48 days. (a) Homogeneous chip of microbial mat of 10 to 20 μm thickness. Cracks are likely artifacts due to sample preparation. (b–d) Fragments of carbonaceous material from a chert band. The thickness and shape of the chips are consistent with those of the dark carbonaceous wisps within the chert bands observed in thin section (Fig. 6). Surfaces of microbial mats under SEM are smooth and bulbous; cross-sectional views show faint internal horizontal lamination resulting from varying porosity.

For carbon isotope analyses ($\delta^{13}C_{org}$), 16 rectangular chips of 1 to 2 cm³ volume each were cut from chert bands in sandstone with a thin water-cooled saw blade to avoid chemical alteration of the chert band composition due to sample heating. The samples also included some sandstone material, whereby sandstone samples free of chert bands were also measured. All samples were washed in alcohol, dried, and ground to powder using an agate mill. Stable isotope analysis and concentration measurements of organic carbon were performed with a THERMO/Finnigan MAT V isotope ratio mass spectrometer, coupled to a THERMO Flash EA 1112 elemental analyzer via a THERMO/Finnigan Conflo III-interface in the stable isotope laboratory of the Museum für Naturkunde, Berlin. Stable isotope ratios are expressed in the conventional delta notation ($\delta^{13}C$) relative to VPDB (Vienna PeeDee Belemnite standard). Standard deviation for repeated measurements of laboratory standard material (peptone) is generally better than 0.15 per mil (‰). Standard deviations of concentration measurements of replicates of the laboratory standard are <3% of the concentration analyzed.

Electron microprobe imaging of rhythmically laminated chert bands was conducted with a JEOL JXA 8200 Superprobe at the Department of Geological Sciences at 15 keV accelerating voltage using the backscatter-electron imaging (BSE) mode.

RESULTS

Silicified Patchy Microbial Mats (Chert Bands)

Chert bands always grade from and into green crinkly laminae. They occur parallel to the bedding plane but are also involved in deformation by fluid escape structures, suggesting a plastic constitution. Chert bands weather resistantly (Fig. 4). Field observations indicate that chert bands generally vary in thickness from 0.1 cm to 0.8 cm (mean 0.3 cm) and reach 4 to 88 cm in length (mean 27 cm). We found no relationship between thickness or length and the stratigraphic position of individual chert bands. Chert bands appear to have preferentially grown above small channel-fill lenses of well-sorted, coarse-grained sandstone. They are in turn sharply overlain by medium- and fine-grained sandstone (Fig. 5).

In thin section, black chert bands consist of several parallel, intensely deformed thin laminations of opaque matter embedded in and separated by a microquartz matrix (Fig. 6). Commonly, single sand grains are observed "floating" surrounded by laminated chert.

HF Etching and Maceration

After 28 days of maceration, the remaining organic material from the chert band samples showed polygonal structures (Fig. 7a–c) and cavities (Fig. 7d) with diameters of ~1 to 2 μm when observed under the SEM.

Substantial quantities of organic material remained after complete maceration of the chert bands. They mostly consisted of pseudo-polygonal chips of uniform thickness of 15 to 20 μm (Fig. 8). These were internally laminated and showed a membrane-like construction. Chip margins were smooth and appeared plain; surfaces were plane or bulbous. The interior of the chip was split by fractures. No partial cell structures or parts thereof were observed.

Raman Spectroscopy

The obtained spectra showed similarities with those of graphitic carbon (Fig. 9a). Colors (Fig. 9b) represent Raman intensities of amorphous carbon. The size, shape, and location of the high-intensity C band on the Raman intensity map (Fig. 9b) correspond to the dark band seen under the petrographic microscope.
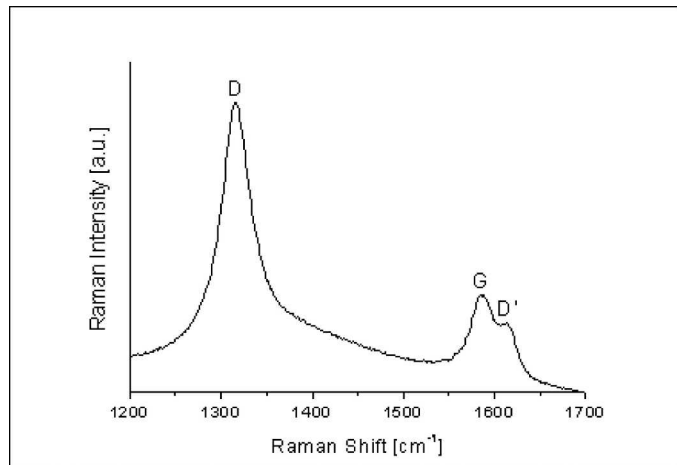
FIG. 9.—(a) Cutout of a Raman spectrum, showing G, D1, and D2 bands. The G ("graphite") peak represents the band distinctive for graphite. The prominent D ("disordered") peaks (D1 and D2) refer to the crystallite size of carbonaceous material (Pasteris and Wopenka 2003).

Organic Carbon Isotopes

The $\delta^{13}C_{org}$ values correspond to the proportion of chert bands in each chip of a bulk-analyzed sandstone-chert sample. Four samples were analyzed and broken into two to five chips each. Figure 10 shows the results from the four chips of sample No. 3. The chip with the highest proportion of chert (upper right) yielded the lowest $\delta^{13}C_{org}$ value and vice versa. This suggests that material with isotopically light C is concentrated in the chert band. The other three samples yielded similar results (Table 2).

Spatial Distribution of Elements

Elemental intensity maps (Fig. 11) clearly demonstrate the mineralogical difference between the chert band and adjacent sandstone by relative enrichment of Li, Mg, and Rb in the sandstone.

Microprobe Imaging

Electron microprobe BSE imaging of multiply laminated black chert showed virtually no backscatter contrast between phases that were clearly discernible in thin section (Fig. 12). Where weakly defined in the BSE image, the laminae appear to be marked by subtle variation in quartz content, which suggests minor differences in cementation. Isolated very small patches of high contrast (black in Fig. 12) are likely pyrite, which was also found by Raman microscopy.

DISCUSSION

Primary Organic Origin and Microscopic Inferences

Our integrated analysis from micrometer (microscopic) to meter (outcrop) scale indicates that the thin laminations within the chert bands are products of Archean microbial mats. The carbonaceous matter in the investigated samples is clearly of primary biogenic origin. There was no observed indication of remobilization, migration, or neomorphism of the organic matter. An abiogenic origin of the crinkly laminations, be it by low-grade alteration or as carbonaceous stylolites, appears highly unlikely because there is no evidence of compaction, evaporitic dissolution, pressure shadow formation, or secondary crystal growth near and in the laminae. Tectonic fabrics are also absent.

The bulbous and domal morphology of the thin, wavy, closely spaced laminations in Moodies sandstones (Fig. 5) resembles that of recent photosynthetic filament–dominated microbial mats in siliciclastic environments (cf. Gerdes et al. 2007 in Schieber et al. 2007).

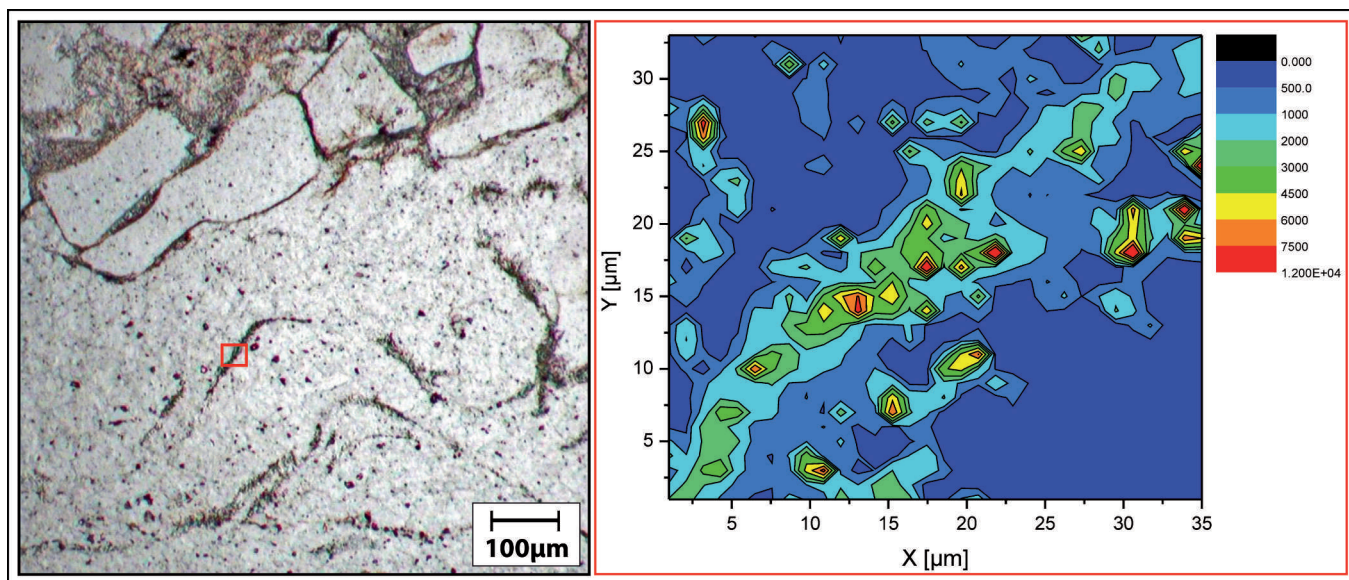SEM images (Figs. 7, 8) show structures consistent in shape and size

FIG. 9.—(b) Photomicrograph of chert band with wisp of dark matter (rectangle; left) and corresponding Raman map of the G band at 1585 cm^{-1} (right). Color scale represents Raman intensities of amorphous carbon. The shape of the anomaly and the corresponding values indicate that the dark wisps consist of organic carbon.
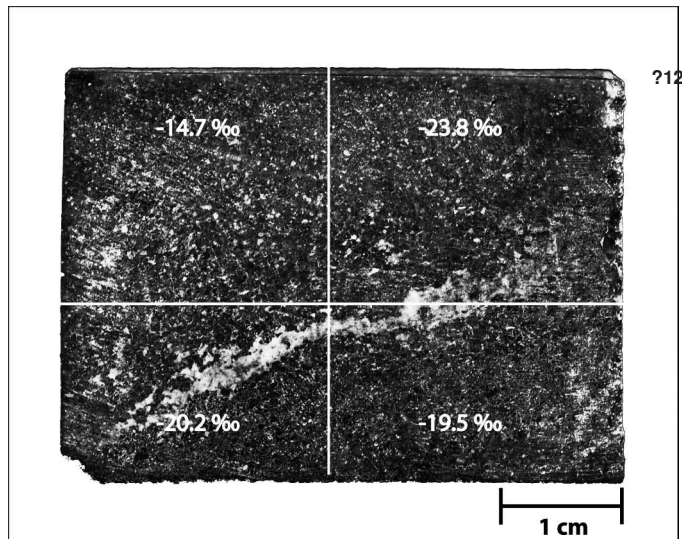
Fig. 10.—Photographs of sample No. 3 divided into four chips, with their respective $\delta^{13}C_{org}$ values posted.

Table 2.—$\delta^{13}C_{org}$ values of four chert-band–bearing sandstones (samples 1–4, MdQ1, member 2), which were each cut into two to five smaller chips.

Sample No.	Chip 1	Chip 2	Chip 3	Chip 4	Chip 5
1	−14,126	−21,675			
2	−23,279	−22,434	−21,853	−23,646	
3	−20,173	−14,667	−19,508	−23,759	
4	−19,942	−20,487	−21,242	−19,361	−20,962

with cells, cell membranes, and former extracellular polymeric substance (EPS). They morphologically resemble coccoid cyanobacteria from Neoarchean carbonates (Kazmierczak et al. 2009). Therefore, these structures are believed to represent early-silicified cell-wall fragments from mat-building organisms. No structures representing filamentous bacteria were observed.

Early Diagenesis and Selective Preservation

Laboratory experiments (Orange et al. 2009) demonstrated that silicification of selected living Archaea (*Methanocaldococcus jannaschii, Pyrococcus abyssi*) in a simulated hydrothermal environment preserved cells of *P. abyssi* but not *M. jannaschii* and incorporated the former gradually in silicifying EPS. By analogy, this experimental outcome may indicate that the Archean microbial community studied here may be similarly complex. This is also consistent with the variation of $\delta^{13}C_{org}$ (Fig. 10) in the sandstone-chert bulk sample and the variable cell morphologies (Fig. 8).

The scarcity of cell structures, concurrent with high Raman intensities of amorphous carbon from chert bands, suggests that the crinkled laminations in Moodies sandstone may represent silicified EPS with diffuse organic carbon. The paucity of grain-to-grain contacts in thin section and the general lack of a diagenetic fabric indicate an early silicification prior to compaction. Because the silicification is not locally restricted but occurs laterally and in several units of the Moodies Group over several kilometres of strike length, a hydrothermal contribution to the silicification process seems unlikely. Silicification was presumably triggered through amorphous-silica–saturated seawater interacting with organic molecules at the seawater–sediment interface, possibly aided by anaerobic bacterial decomposition of organic matter (Lowe and Byerly 1999). High Li, Mg, and Rb values in the sandy host rock material, shown in the LIBS maps, are relative enrichments expected for K-feldspar– and mica-bearing sandstones. Their strong relative depletion in the chert bands attests to the near-absence of postdepositional geochemical reequilibration.

IMPLICATIONS

The crinkled laminations and chert bands in Moodies Group sandstones represent the oldest well-preserved widespread siliciclastic Archean microbial mats. The structures preserved in chert bands likely represent former cells or cell fragments and EPS and pass the criteria for syngeneity and biogenicity (Altermann 2001, Altermann and Kazmierczak 2003, Brasier et al. 2006). Associated sedimentary structures can be field-mapped over extensive distances and correlate with facies changes and environmental gradients (e.g., water depth, nutrient levels; Heubeck 2009). At hand sample scale, C_{org}-coated surfaces form complex, similarly shaped domal and bulbous forms, which interact with current-shaped sedimentary structures, suggesting plastic behavior, which is common for microbial communities. SEM photographs show fossil cell morphologies; carbon isotopic analyses suggest the presence of biologically mediated material and the absence of minerals commonly formed during hydrothermal or tectonic processes.

Selective preservation of cell structures, variability of $\delta^{13}C_{org}$ in bulk samples, and the macroscopic morphological variety of the crinkly laminae, in combination with evidence for adaptation to highly variable sedimentary dynamics (Heubeck 2009), suggest that these microbial mats showed a high degree of complexity and hint at earlier steps in organismic evolution, as previously suggested (Orange et al. 2009).

The mappable extent of the macroscopically visible microbial mats, ubiquitously preserved in millimeter- and centimeter-spaced, green wispy laminations and chert bands over a section hundreds of meters thick and extending over many kilometers along strike, implies rapid growth rates of microbial mats fueled by an ample supply of nutrients and a high resilience against environmental changes. They constitute a surprisingly large volume of benthic biomass. If Archean siliciclastic shorelines in general had a similar appearance as the occurrence studied here, microbial mats would have exerted major influence on shoreline morphology and sediment dynamics.

If microbial mats became silicified while still exposed at the sediment–water or sediment–atmosphere interface, they likely acted as an effective barrier between unconsolidated sediment and the flowing, sediment-laden water. The implications of this effect are to-date poorly known but, aside from the well-documented retarded dewatering, may have included a reduced surface roughness to turbulent flow and a longer residence time of saturated interstitial waters, thus affecting weathering and early diagenesis.

The $\delta^{13}C$ values lie within the range of recent marine photosynthesizers and thus also make a significant contribution by (strongly $\delta^{13}C$-negative) methanotrophs unlikely. Even though the microbial mat morphology resembles that of modern photosynthetic mats, we know that this is an indirect argument at best. There is no attempt to relate the detected structures to a specified group of organisms.

CONCLUSIONS

We concluded that the black chert bands and, by extension, also the abundant green crinkly mats, are moderately to excellently preserved
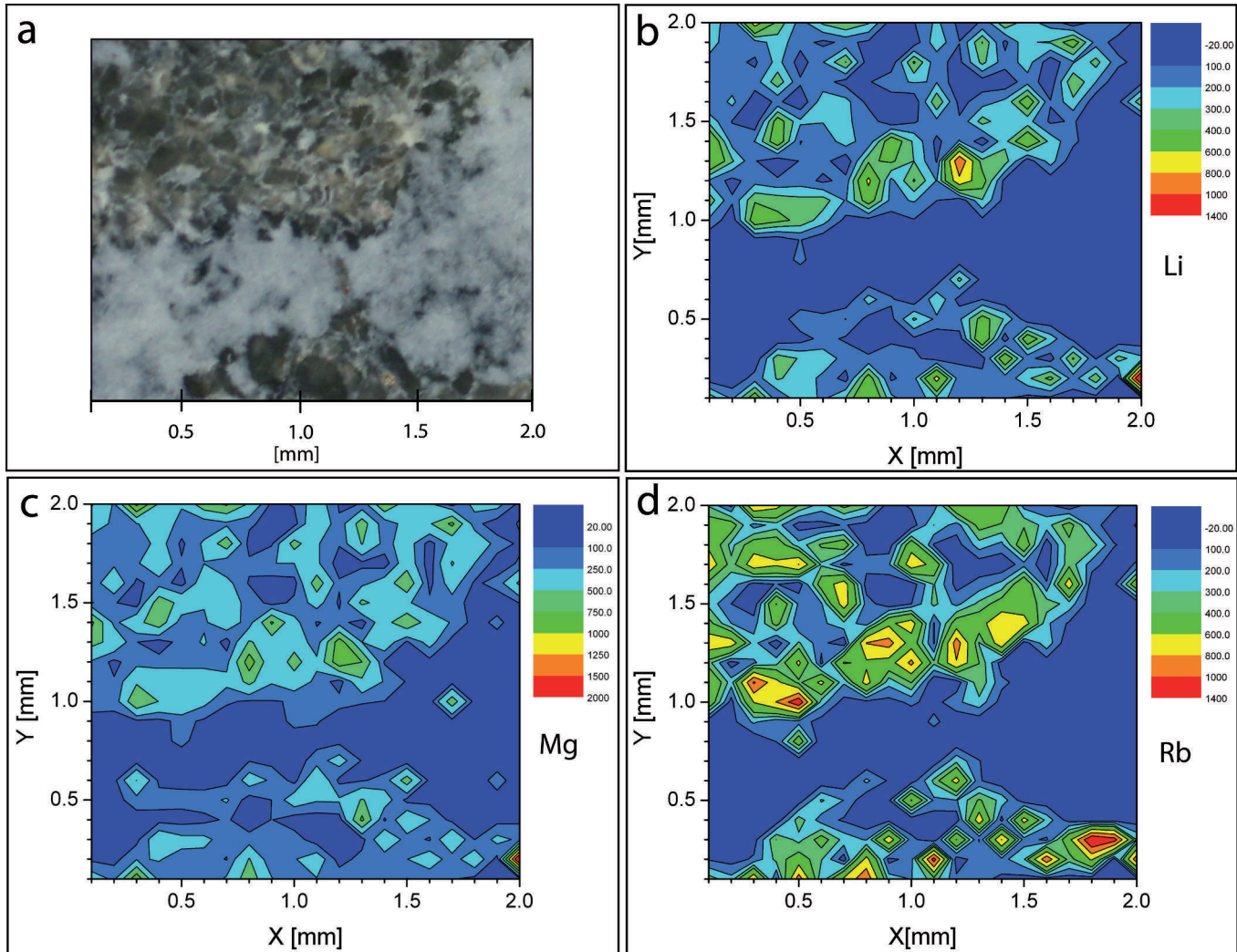
FIG. 11.—LIBS maps of Li, Mg, and Rb presenting elemental intensities of the area shown in the thin-section photomicrograph. (a) Polarized light photomicrograph of the mapped area. The chert band (white) crosses the picture from the lower left to the upper right, surrounded by sandstone (dark). (b–d) Intensity maps for Li, Mg, and Rb demonstrating a relative enrichment of these elements in the sandstone, whereas the chert band is characterized by relative depletion.
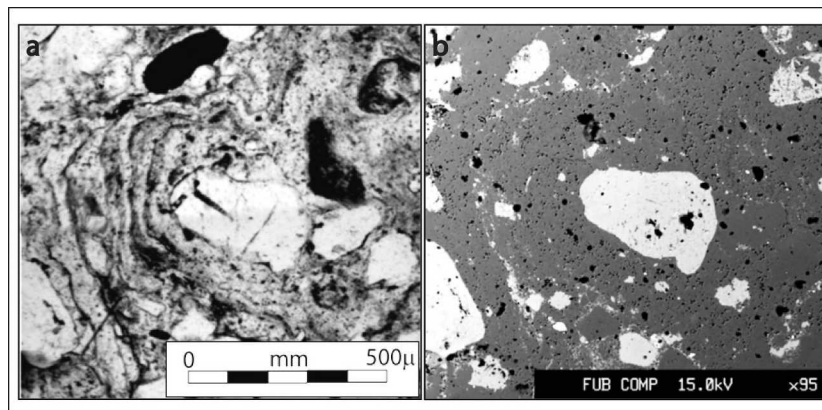

FIG. 12.—BSE image of stacked carbonaceous laminae in chert overgrowing "floating" sand grain (center). Feldspar grains are shown in white; quartz is shown in dark gray. The layering defined by contrasting composition is clearly visible in petrographic thin section (a) but invisible in the BSE image (b), suggesting a carbonaceous composition of the dark bands. Thin section 848–1.

microbial mats of unknown metabolism. Anoxygenic or oxygenic photosynthesizing or even heterotroph and complex microbial mats comparable to some modern analogs (Noffke et al. 2003, Schieber et al. 2007) may be reasonably inferred. Their widespread occurrence in medium- to high-energy shoreline settings across the Moodies stratigraphic record attests to the adaptability and tenacity of microbial life in the Middle Archean.

ACKNOWLEDGMENTS

REFERENCES

Allwood AC, Walter MR, Burch IW, Kamber BS. 2007. 3.43 billion-year-old stromatolite reef from the Pilbara Craton of Western Australia: ecosystem-scale insights to early life on Earth. *Precambrian Research* 158:198–227.

Altermann W. 2001. The oldest fossils of Africa—a brief reappraisal of reports from the Archean. *Journal of African Earth Sciences* 33:427–436.

Altermann W, Kazmierczak J. 2003. Archean microfossils: a reappraisal of early life on Earth. *Research in Microbiology* 154:611–617.

Anhaeusser CR. 1975. The Geological Evolution of the Primitive Earth: Evidence from the Barberton Mountain Land: Economic Geology Research Unit, University of the Witwatersrand, Johannesburg, South Africa, Info Circular No. 98, 22 p.

Anhaeusser CR. 1976. The geology of the Sheba Hills area of the Barberton Mountain Land, South Africa, with particular reference to the Eureka Syncline. *Geological Society of South Africa Transactions* 79:253–280.

Brandl GM, Cloete M, Anhaeusser CR. 2006. Archaean greenstone belts. *In* Johnson MR, Anhaeusser CR, Thomas RJ (Editors). *The Geology of South Africa*: Geological Society of South Africa and Council of Geoscience, Johannesburg/Council for Geoscience, Pretoria. p. 9–56.

Brasier M, McLoughlin N, Green O, Wacey D. 2006. A fresh look at the fossil evidence for early Archean cellular life. *Philosophical Transactions of the Royal Society, Series B* 361:887–902.

de Ronde CEJ, de Wit MJ. 1994. Tectonic history of the Barberton Greenstone Belt, South Africa: 490 million years of Archean crustal evolution. *Tectonics* 13(4):983–1005.

Eriksson KA. 1977. Tidal deposits from the Archaean Moodies Group, Barberton Mountain Land, South Africa. *Sedimentary Geology* 18:257–281.

Eriksson KA. 1978. Alluvial and destructive beach facies from the Archaean Moodies Group, Barberton Mountain Land, South Africa and Swaziland. *In* Miall AD (Editor). *Fluvial Sedimentology*: Canadian Society of Petroleum Geology, Calgary, Canada. Memoir 5, p. 287–311.

Eriksson KA. 1979. Marginal marine depositional processes from the Archaean Moodies Group, Barberton Mountain Land, South Africa: Evidence and significance. *Precambrian Research* 8:153–182.

Eriksson KA. 1980. Transitional sedimentation styles in the Fig Tree and Moodies Group, Barberton Mountain Land, South Africa: evidence favoring an Atlantic or Japan Sea–type Archean continental margin. *Precambrian Research* 12:141–160.

Eriksson KA, Simpson E. 2002. Quantifying the oldest tidal record: the 3.2 Ga Moodies Group, Barberton Greenstone Belt, South Africa. *Geology* 28:831–834.

Eriksson KA, Simpson EL, Mueller W. 2006. An unusual fluvial to tidal transition in the Mesoarchean Moodies Group, South Africa: a response to high tidal range and active tectonics. *Sedimentary Geology* 190:13–24.

Hall AL. 1918. *The Geology of the Barberton Gold Mining District*: Geological Survey of South Africa. Pretoria. Memoir 9, 347 p.

Heubeck C. 2009. An early ecosystem of Archean tidal microbial mats (Moodies Group, South Africa, ca. 3.2 Ga). *Geology* 37(10):931–934.

Heubeck C, Lowe DR. 1994a. Depositional and tectonic setting of the Archean Moodies Group, Barberton Greenstone Belt, South Africa. *Precambrian Research* 68:257–290.

Heubeck C, Lowe DR. 1994b. Late syndepositional deformation and detachment tectonics in the Barberton Greenstone Belt, South Africa. *Tectonics* 13:1514–1536.

Heubeck C, Lowe DR. 1999. Sedimentary petrology and provenance of the Archean Moodies Group, Barberton Greenstone Belt, South Africa. *In* Lowe DR, Byerly GR (Editors). *Geology of the Barberton Greenstone Belt, South Africa*: Geological Society of America, Boulder, Colorado. Special Paper 329, p. 259–287.

Heubeck C, Lowe DR, Byerly GR. 2010. High but balanced sedimentation and subsidence rates (Moodies Group, Barberton Greenstone Belt), followed by basin collapse: implication for Archaean tectonics. *Geophysical Research Abstracts* 12:6260.

Hoehse M, Mory D, Florek S, Weritz F, Gornushkin I, Panne U. 2009. A combined laser-induced breakdown and Raman spectroscopy Echelle system for elemental and molecular microanalysis. *Spectrochimica Acta Part B* 64:1219–1227.

Javaux EJ, Marshall CP, Bekker A. 2010. Organic-walled microfossils in 3.2-billion-year-old shallow-marine siliciclastic deposits. *Nature* 463:934–938.

Kazmierczak J, Altermann W, Kremer B, Kempe S, Eriksson PG. 2009. Mass occurrence of benthic coccoid cyanobacteria and their role in the production of Neoarchean carbonates of South Africa. *Precambrian Research* 173:79–92.

Lowe DR, Byerly GR (Editors). 1999. *Geologic Evolution of the Barberton Greenstone Belt, South Africa*: The Geological Society of America, Boulder, Colorado. Special Paper 329, 319 p.

Lowe DR, Byerly GR. 2007. An overview of the geology of the Barberton Greenstone Belt and vicinity: implications for early crustal development. *In* van Kranendonk M, Smithies H, Bennett V (Editors). *Earth's Oldest Rocks*: Elsevier, Amsterdam. Developments in Precambrian Geology 15, p. 481–526.

Marshall CP, Love GD, Snape CE, Hill AC, Allwood AC, Walter MR, Van Kranendonk MJ, Bowden SA, Sylva SP, Summons RE. 2007. Structural characterization of kerogen in 3.4 Ga Archean cherts from the Pilbara Craton, Western Australia. *Precambrian Research* 155:1–23.

Noffke N, Eriksson KA, Hazen RM, Simpson EL. 2006. A new window into Early Archean life: microbial mats in Earth's oldest siliciclastic tidal deposits (3.2 Ga Moodies Group, South Africa). *Geology* 34(4):253–256.

Noffke N, Gerdes G, Klenke T. 2003. Benthic cyanobacteria and their influence on the sedimentary dynamics of peritidal depositional systems (siliciclastic, evaporitic salty, and evaporitic carbonatic). *Earth-Science Reviews* 62:163–176.

Ohnemueller F, Heubeck C, Kirstein J, Gamper A. 2010. A basin on an unstable ground: correlation of the Middle Archean Moodies Basin, Barberton Greenstone Belt, South Africa. *Geophysical Research Abstracts* 12:5267.

Orange F, Westall F, Disnar J-R, Prieur D, Bienvenu N, Le Romancer M, Défarge CH. 2009. Experimental silicification of the extremophilic Archaea Pyrococcus abyssi and Methanocaldococcus jannaschii: applications in the search for evidence of life in early Earth and extraterrestrial rocks. *Geobiology* 7:403–418.

Pasteris JD, Wopenka B. 2003. Necessary, but not sufficient: Raman identification of disordered carbon as a signature of ancient life. *Astrobiology* 3(4):727–738.

Schieber J, Bose PK, Eriksson PG, Banerjee S, Sarkar S, Altermann W, Catuneanu O. 2007. *Atlas of Microbial Mat Features Preserved within the Siliciclastic Rock Record*, Atlas in Geosciences 2: Elsevier Amsterdam. 311 p.

Sugitani K, Lepot K, Nagaoka T, Mimura K, Van Kranendonk M, Oehler DZ, Walter MR. 2010. Biogenicity of morphologically diverse carbonaceous microstructures from the ca. 3400 Ma Stelley Pool Formation, in the Pilbara Craton, Western Australia. *Astrobiology* 10(9):899–920.

Ueno Y, Isozaki Y, Yurimoto H, Marayuma H. 2001. Carbon isotopic signatures

of individual Archean microfossils(?) from Western Australia. *International Geology Review* 43:196–212.

Visser DJL (Editor), with reports by Eeden OR, van Joubert GK, Söhnke APG, Zyl JS, van Roussow PJ, Taljaard JJ, Visser DJL. 1956. *The Geology of the Barberton Area*: Geological Survey of South Africa, Pretoria. Special Publication 15.